High-Gain Persistent Nonlinear Conductivity in High-Voltage Gallium Nitride Photoconductive Switches

E. A. Hirsch, A. Mar, F. J. Zutavern, G. Pickrell, J. Delhotal, R. Gallegos, V. Bigman
Sandia National Laboratories
Albuquerque, New Mexico, USA

J. D. Teague, J. M. Lehr
Department of Electrical and Computer Engineering
University of New Mexico
Albuquerque, New Mexico, USA

***Abstract*— Wide-bandgap GaN optically-controlled switches have the potential for driving down the cost and size and improving the efficiency and capabilities of high voltage pulsed-power applications. Key to these applications is the understanding of the high-field photo-conductive properties of this material to determine if it will operate in a high-gain and/or sub-bandgap triggering mode, such as has been observed in GaAs. Photoconductive semiconductor switches (PCSS) were fabricated and tested from GaN wafers from Kyma Technologies and Ammono. With relatively low voltages applied the switch, linear photoconductive currents are measured in response to exposure to laser pulses of sub-bandgap wavelength (532 nm). Above a threshold voltage applied to the PCSS, persistent conductivity is measured that lasts well beyond the duration of the laser pulse and discharges the charged transmission line in the system. The sustaining field for this switching mode is approximately 3kV/cm. Another known distinguishing characteristic of high-gain switching is the formation of filamentary current channels that can be imaged due to the emission of recombination radiation from the plasma within the filaments. These filaments have been also observed in the GaN switches. High-gain switching has been initiated in GaN devices with as little as 2.5 μJ laser energy. This persistent photoconductivity is a distinguishing characteristic of what is known as "lock-on" effect most notably known in GaAs-based photoconductive switches, and is the basis for highly-efficient photoconductive switching requiring relatively little laser energy.**

***Keywords*—lock-on; photoconductive semiconductor switch; gallium arsenide; gallium nitride; photoconductive switching; wide-bandgap**

I. INTRODUCTION

There is a vast need for fast high voltage switches to be used in power electronics and pulsed power applications. Wide bandgap (WBG) semiconductor materials have multiple advantages over typical semiconductors that have helped significantly advance high voltage switching over the last decade [1]. Table 1 shows the superior material properties of SiC and GaN to Si or GaAs for high voltage switching, namely their wide bandgap and breakdown field. GaN, specifically, has the largest bandgap, which results in less thermally generated carriers, a high breakdown field, which results in smaller device widths for similar breakdown voltages in Si or GaAs devices, and a mid-range thermal conductivity, which allows for elevated temperature operation of GaN PCSS. These parameters lead towards smaller systems with smaller devices and lesser thermal management requirements.

Wide bandgap semiconductor switches have been researched with various materials (SiC, GaN, etc.) and various transistors (diodes, MOSFETs, IGBTs, thyristors, HEMTs, etc.). Typical state of the art WBG MOSFETs have a switching time in the hundreds of nanoseconds to tens of microseconds, but PCSS switches could switch in the single to tens of nanoseconds range, which allows for higher frequency switching in power electronics applications and decreases the physical size of components in the system [2-5]. State of the art switches in the market today can hold off approximately 15-20 kV and to reach the required high voltage hold off typical of power electronics for dc transmission, multiple switches need to be stacked in series, which comes with complex gate drive systems, whereas photoconductive semiconductor switches are optically controlled, which removes the requirement of floating gate driver systems [1].

GaAs PCSS exhibit a high-gain triggering mode above 4-6 kV/cm [2]. This is believed to be a low-field avalanche carrier generation mode, which has demonstrated up to 10^5 times as many carriers produced by the electric field as created by the optical trigger in low-impedance circuits. This feature provides a tremendous reduction in the optical trigger energy required to activate the switch, increasing switch efficiency. In this mode, the PCSS will also continue to conduct if the field across the switch (provided by the external circuit) remains greater than 4-6 kV/cm, allowing switch triggering with nanosecond long optical pulses. SNL has observed high-gain triggering in GaAs and InP, but not in Si, SiC, GaP, or C (diamond). GaAs and InP are direct-bandgap semiconductors, while the others are indirect-bandgap. All insulating or semi-insulating materials will exhibit avalanche carrier generation at high fields (> 200 kV/cm). The unusual property of GaAs and InP is that they exhibit avalanche carrier generation when optically triggered at low fields (< 10 kV/cm).

Another significant feature, sub-bandgap triggering, has been demonstrated in GaAs and allows triggering with long wavelength lasers, e.g. 1064 nm from Nd:YAG lasers [3]. Sub-bandgap radiation is absorbed less efficiently than above-bandgap radiation, but high-gain triggering more than compensates for the less-efficient absorption (and losses in wavelength conversion). The absorption depth at 800 nm (the bandgap of GaAs corresponds to 875 nm) is less than 1 μm, whereas the absorption depth at 1064 nm depends on the defect density, but is typically greater than 1 cm. This longer absorption depth has the advantage that photo-carriers can be generated throughout the thickness of the substrate, such as in vertical structures, so the location of avalanche carrier generation can be initiated in high-field regions in the bulk of the device, away from low-field breakdown strength surfaces. This allows for device electric field hold-off to approach the ideal bulk breakdown strength, which is much higher than of surface interfaces.

Like GaAs, GaN and AlGaN alloys are direct-bandgap semiconductors. This does not guarantee that they will exhibit high-gain or sub-bandgap triggering, but does suggest distinct possibilities that merit determination. If GaN and/or AlGaN alloys exhibit high-gain or sub-bandgap triggering, PCSS devices from these materials will be designed to make use of these effects and will greatly outperform either conventional Si or GaAs PCSS. In particular, the high-field strength properties of GaN would be a key enabler for sub-bandgap triggered vertical structures for high-voltage 2-D current-sharing filament arrays limited by the voltage breakdown of conventional thickness substrates [3]. If either or both of these effects are not exhibited, then the other properties of these WBG semiconductors, e.g. higher electric field hold-off, faster recovery, and higher temperature operation, still imply significantly better PCSS properties than are available from silicon or GaAs.

II. Device Fabrication and PCSS Device Properties

A. Device Fabrication Overview

Semi-insulating GaN wafers were received from Kyma Technologies and Ammono. The Kyma Technologies wafer material is research grade semi-insulating GaN grown by HVPE. Figure 1(a) shows a number of surface defects visible by eye. The wafers are provided in 10 mm x 10 mm size with a thickness of approximately 475 μm. The resistivity of the Kyma wafers is quoted to be greater than 10^6 Ω-cm and the dislocation density is quoted to be less than 5×10^6 cm^2. The Ammono wafer material is semi-insulating GaN using ammonothermal growth. There are no large defects seen on the surface, as shown with Figure 1(b). The Ammono wafers were provided in 37.9 mm diameter wafers with a thickness of approximately 350 μm. The resistivity of the Ammono wafers is quoted to be greater than 10^9 Ω-cm with a dislocation density less than 5×10^4 cm^2.

TABLE I. Material Properties Comparison

Properties	**Si**	**GaAs**	**4H SiC**	**GaN**
Bandgap (eV)	1.11	1.43	3.26	3.42
Dielectric constant	11.8	12.8	9.7	9
Breakdown field (MV/cm)	0.25	0.35	3.5	3.5
Thermal conductivity (W/cm*K)	1.5	0.46	4.9	1.7

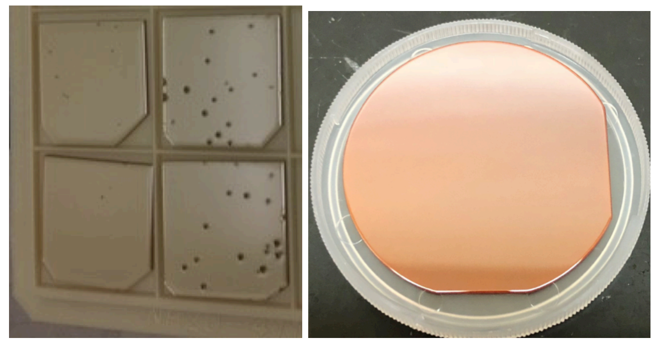

(a) (b)

Fig. 1. Example wafers from (a) Kyma Technologies and (b) Ammono.

The first wafer mask design was targeted towards test of the material properties of the GaN from each manufacturer. Ti/Al/Ni/Au alloy and Ti/Au bondpad metal layers were deposited on the wafer and patterned to form n-type contacts. The wafer was split into a wafer probe section and singulated die section with gap spacings of 25, 50, 100, 300, and 600 μm in the wafer probe section and 12 devices with 600 μm gap spacing in the singulated die section. Figure 2 shows a 600 μm gap singulated device with two gold ribbons bonded to each electrode. The singulated die was ribbon bonded to test boards for in-circuit testing and the wafer probe section was used to test multiple material parameters, such as the dark leakage current and surface flashover electric field of the material.

B. Dark Leakage Current

The devices were tested for their leakage current during voltage holdoff without laser light illuminating the device gap, to measure “dark” leakage current. Devices made from both manufacturers were tested and compared. Figures 3 and 4 below show the leakage current for two each of Ammono and Kyma devices. The Ammono devices were tested with a 3 kV, low current I-V curve tracer since they had leakage current in the tens of picoamperes. The Kyma devices were tested with fluorinert covering the top of the device up to 10 kV with a higher current IV curve tracer. As shown in Figures 3 and 4, the Ammono devices have approximately 4 - 5 orders of magnitude better off state resistance than the Kyma devices.

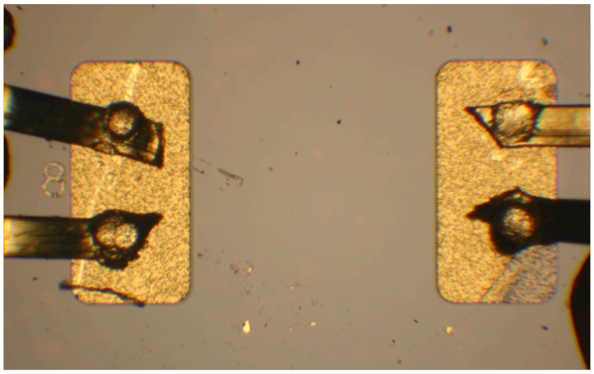

Fig. 2. Kyma PCSS singulated device die.

C. *Surface Flashover Electric Field*

The maximum high-voltage holdoff of lateral configuration PCSS switches is limited by the surface breakdown strength between the electrodes, particularly when the devices are tested in air. The dielectric strength of the devices varies depending on the high voltage pulse width, but in air the Kyma Technologies and Ammono devices had a surface flashover electric field of approximately up to 40 kV/cm for 500 ns pulse duration. When immersed in fluorinert FC-70, no breakdown was observed up to the maximum 600 kV/cm measurement limit for pulses of up to 5 µs duration.

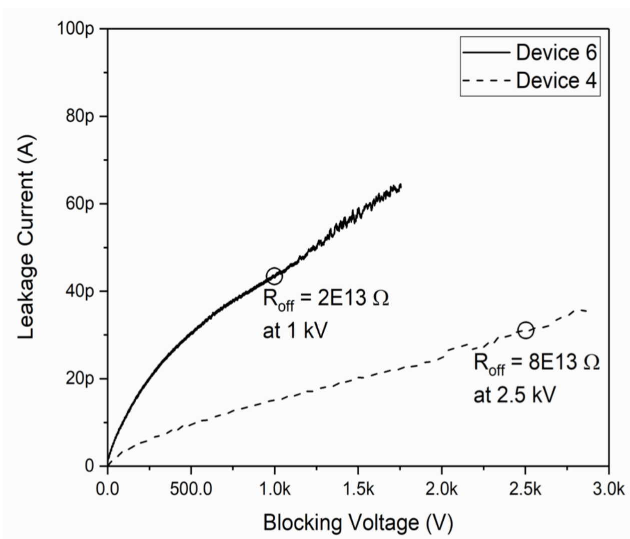

Fig. 3. Ammono PCSS dark leakage current.

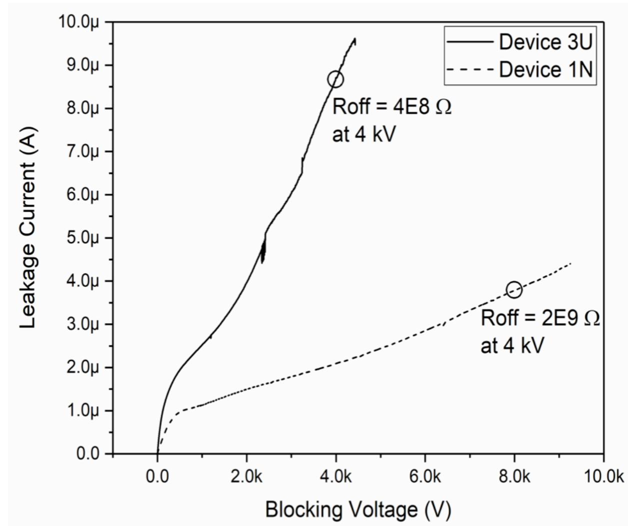

Fig. 4. Kyma PCSS dark leakage current.

III. PCSS TEST CONFIGURATION

The PCSS devices were tested in the circuit depicted in Figure 5. A dc power supply charged a DEI pulse generator to between 0 V – 2500 V. The DEI pulse generator was controlled with a DG535 delay generator to pulse charge a diode chain and short RG-214 cable with approximately a 60 ns rise / fall time. A frequency doubled Nd:YAG Q-switched laser with a 6 ns pulse width was used as the optical trigger to the PCSS. The testing thus far on the PCSS devices has been conducted at the sub-bandgap wavelength of 532 nm (bandgap wavelength is 365 nm). A 1 kΩ load resistance was used to limit the conduction current through the device below 2 A. A majority of the testing was performed with peak currents between 1 A and 1.5 A. Some testing was done in a single shot configuration, while a majority of the testing was performed at either 1 Hz or 20 Hz repetition rate testing.

The charge voltage, 1 kΩ load voltage, and 0.025 Ω CVR voltage were all recorded throughout testing. A color vision camera took images of the device during conduction to document filamentation and a photodetector recorded the timing of the laser pulse to the current conduction. Separate measurements of laser energy were measured prior to testing the devices.

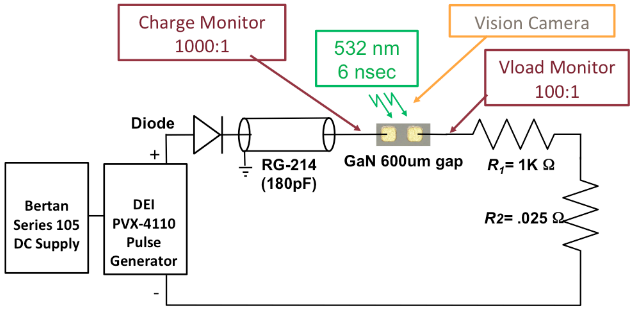

Fig. 5. PCSS test configuration.

IV. PCSS Test Results and Discussion

The GaN PCSS exhibits both linear and high-gain mode switching characteristics. The waveforms presented in Figures 6 and 7 show the linear and high-gain mode switching characteristics, respectively.

The PCSS exhibits linear switching in Figure 6 where the current waveform follows the laser pulse with fast current decay governed by carrier recombination. The charge voltage on the high side of the device has a slight droop, as little of the energy from the transmission line was discharged through the device in the approximately 25 ns long current pulse. The peak current during linear mode operation is only 110 mA.

High gain mode switching is demonstrated in Figure 7. Once lock-on is initiated from laser generated electron-hole pairs, avalanche carrier generation is sustained to maintain conduction even after the laser illumination is removed. The rise time of the current is similar to that of the trigger laser pulse, ~5ns. The switch then remains in the on state until the electric field across the device decays below the minimum critical lock-on field of approximately 3 kV/cm (200 V) as depicted in Figure 7. After the laser illumination is removed, the device remains conducting for an additional 410 ns and is on until the voltage on the high side of the device decays to 200 V. At this point, the conduction current drops to 0 A and the voltage across the device is maintained, indicating that the device has turned off. In switching applications, the remaining unswitched voltage represents a switching loss that can be minimized by operating the switch at as high a field as possible compared to the lock-on field. In the case of the GaN PCSS switching with high-gain in air (breakdown >30 kV/cm), this voltage loss (sustaining field ~3kV/cm) can be less than 10%.

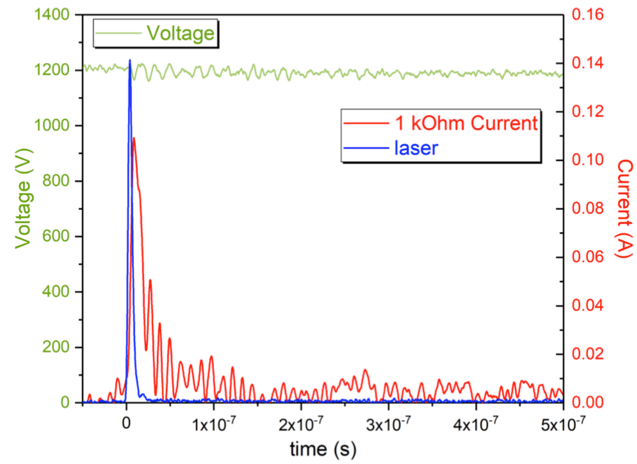

Fig. 6. Example linear mode switching waveform for a GaN PCSS.

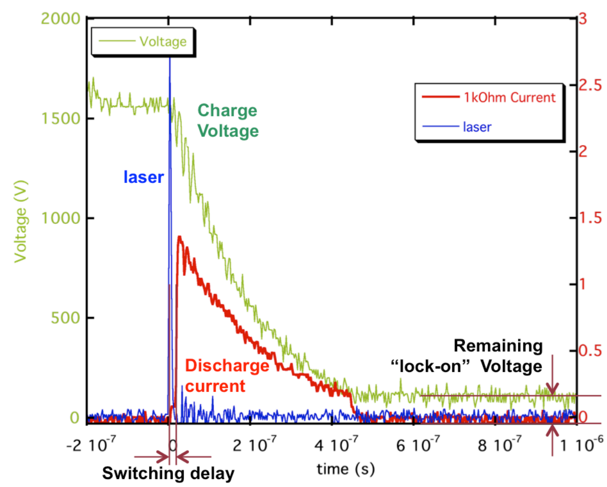

Fig. 7. Example high gain switching waveform for a GaN PCSS.

This non-linear switching has been demonstrated in GaN PCSS to be repeatable and laser induced in all our testing. However, this phenomenon has not yet been demonstrated with fluorinert covering the gap of the device. It has only occurred when the gap of the device is open to the air. This lends to the belief that in GaN, the high-gain mode switching is partially due to a surface effect that is not present when the device is submerged in fluorinert. Further investigation is ongoing to completely understand this mode of operation.

For applications, a key aspect of high gain mode is the reduction in laser energy required to turn on the device. This is significant because it can greatly reduce the size of the laser and driver used for turning on the PCSS. Instead of an Nd:YAG Q-switched laser, a laser diode could be enough energy to drive the semiconductor. In testing, the linear mode switching was initiated with 100 µJ of laser energy and delivered 3.5 µJ of energy to the load, requiring more energy to turn on the device than was delivered. The high gain mode switching in Figure 7 was initiated with 33 µJ of laser energy and delivered 256 µJ of energy to the load, requiring much less energy to turn the device on than was delivered to the load. This allows for much more energy efficient switching with the additional benefit of smaller lasers. Note that the blue laser waveform in Figures 6 and 7 only show the timing of the laser pulse and does not indicate the laser energy.

Filamentary current conduction paths is another distinguishing characteristic of high-gain mode operation of PCSS [2]. Linear mode operation is characterized by uniform conduction across the device, whereas high-gain mode causes filaments, or current channels, to form on the surface of and into the bulk of the device.

The filamentary current channels in high-gain mode can be imaged due to the emission of recombination radiation from the plasma within the filaments. Filamentation has been observed in the GaN PCSS devices during high-gain mode switching. Figure 8 shows the filamentation in the device during the Figure 7 cycle as seen with a color sensitive video camera. As shown, there is a main filament that runs from each electrode of the device towards the right hand side. This filamentation can degrade the device significantly, as has been shown in GaAs PCSS devices [3,8], however, with GaN devices operating at low current conduction of approximately 1 A, the device has been tested to withstand hundreds of pulses.

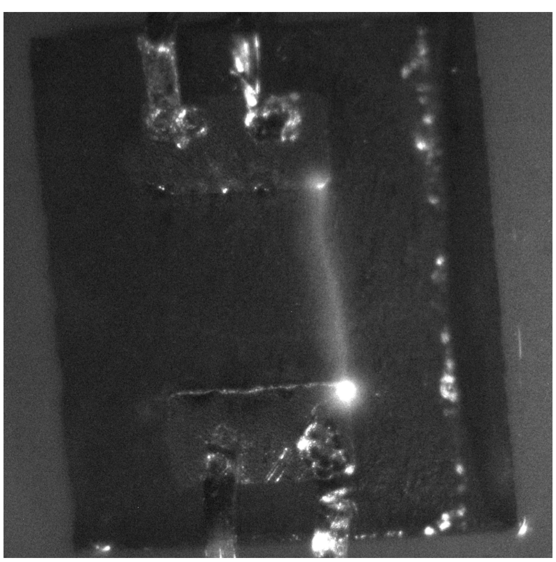

Fig. 8. Filamentary current conduction during a high gain mode switching

V. SWITCHING CHARACTERISTICS – DELAY AND JITTER

While linear conduction in a PCSS is almost instantaneous with laser excitation, high-gain switching typically exhibits some latency between trigger laser absorption and on-state conduction (Figure 7). This delay is associated with the filament formation process that forms the current channel(s) that closes the switch. Stochastic variability associated with impact ionization avalanche carrier generation also leads to timing jitter in high-gain switching. This switching delay and timing jitter are important switching characteristics that are important to understand in considering the use of switches for power electronics applications.

Switching delay and timing jitter are highest at the minimum optical trigger energy and decrease as trigger energy is increased. As shown in figure 9, this characteristic was quantified by compiling time delay and variability statistics for a fixed switching voltage of 2 kV with a 600 µm gap switch while varying optical trigger energy (30 shots per energy level).

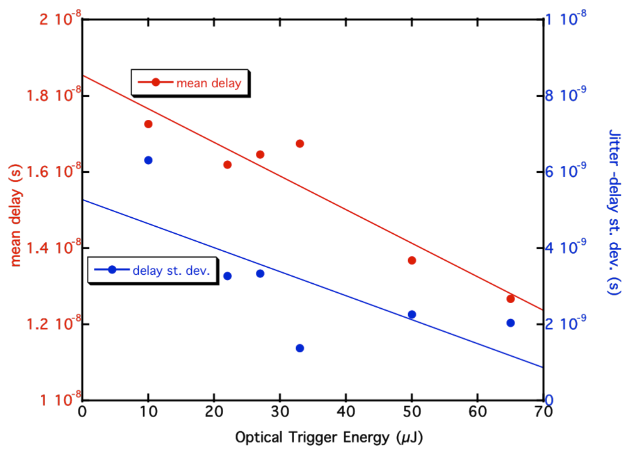

Fig. 9. Optical trigger energy dependence of switching delay and timing jitter in a 600 µm gap GaN PCSS.

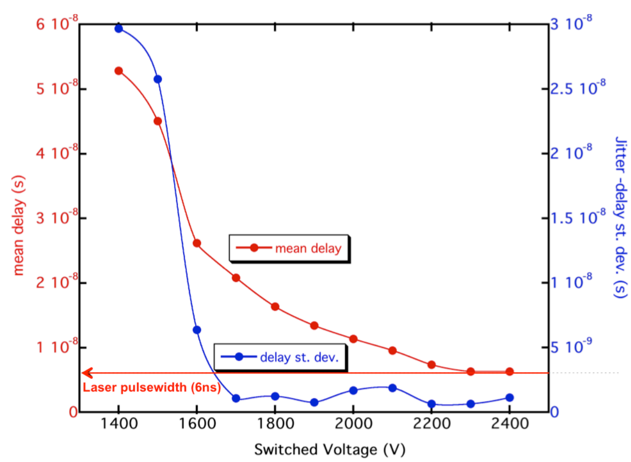

Fig. 10. Switched voltage dependence of switching delay and timing jitter in a 600 µm gap GaN PCSS.

Switching delay and jitter are more strongly dependent on the switched voltage. This dependence was characterized by appling a fixed optical trigger energy of 50 µJ to the 600 µm gap PCSS and varying the switched voltage (60 pulses per voltage level). At lower voltages, the delay is 10s of ns although low (~1ns) jitter is achieved with as low as 1700V applied voltage. At the highest voltages applied (40 kV/cm) the switching delay decreases assymptotically to the laser pulsewidth itself.

VI. CONCLUSION

GaN PCSS devices are a promising technology for repetitive power electronics or pulsed power applications. The material properties of GaN allow for higher voltage and more temperature robust devices. The ability for these devices to be switched in a high gain mode, where persistent conductivity occurs, allows for the use of smaller laser systems and more efficient device triggering. A GaN PCSS research grade device has been tested with over 900 low current (less than 1.5 A peak) 400 ns width pulses, which shows that it could be feasible to use in systems in the future. Some repetitive rate testing at 20 Hz has been accomplished to start testing the low current lifetime of these devices (Figure 11).

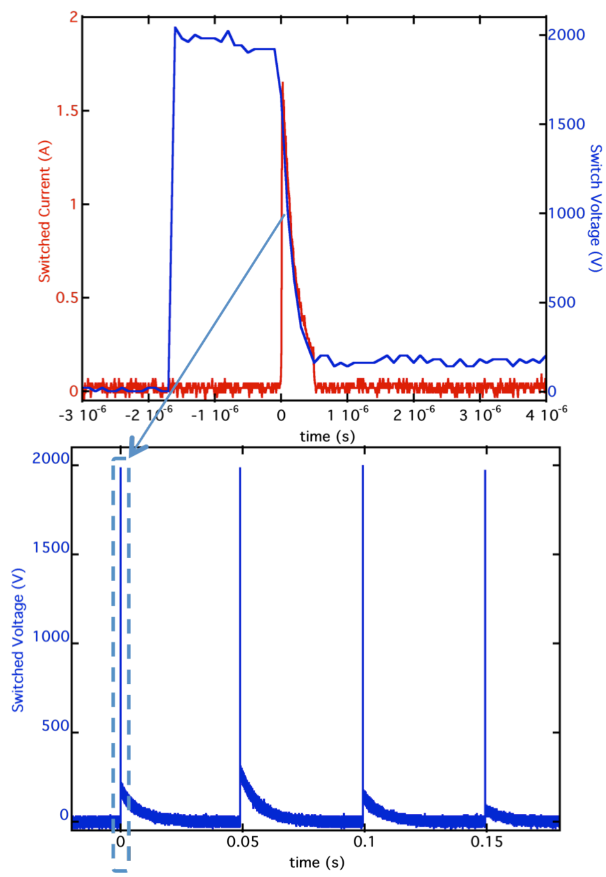

Fig. 11. 20 Hz repetitive high-gain switching of a GaN PCSS.

ACKNOWLEDGMENT

This work was supported by an Advanced Research Projects Agency-Energy (ARPA-E) Innovative Development in Energy-Related Applied Science (IDEAS) project.

Sandia National Laboratories is a multimission laboratory managed and operated by National Technology & Engineering Solutions of Sandia, LLC, a wholly owned subsidiary of Honeywell International Inc., for the U.S. Department of Energy's National Nuclear Security Administration under contract DE-NA0003525. This paper describes objective technical results and analysis. Any subjective views or opinions that might be expressed in the paper do not necessarily represent the views of the U.S. Department of Energy or the United States Government.

REFERENCES

[1] A. V. Bilbao *et al.*, "Continuous switching of ultra-high voltage silicon carbide MOSFETs," *2016 IEEE International Power Modulator and High Voltage Conference* (IPMHVC), San Francisco, CA, 2016, pp. 463-466.

[2] F. Zutavern, S. Glover, K. Reed, M. Cich, A. Mar, M. Swalby, T. Saiz, M. Horry, F. Gruner and F. White, "Fiber-optically controlled pulsed power switches," *IEEE Trans. Plasma Sci*, vol. 36, no. 5, pp. 2533-2540, 2008.

[3] A. Mar, F. Zutavern, G. Vawter, H. Hjalmarson, R. Gallegos and V. Bigman, "Electrical Breakdown Physics in Photoconductive Semiconductor Switches," Sandia National Laboratories, *SAND2016-0109*.

[4] D. L. Mauch et al., "Ultrafast Reverse Recovery Time Measurement for Wide-Bandgap Diodes," in *IEEE Transactions on Power Electronics*, vol. 32, no. 12, pp. 9333-9341, Dec. 2017.

[5] E. A. Hirsch, J. A. Schrock, S. B. Bayne, H. O'Brien and A. Ogunniyi, "Narrow pulse evaluation of 15 KV SiC MOSFETs and IGBTs," *2017 IEEE 21st International Conference on Pulsed Power (PPC)*, Brighton, 2017, pp. 1-4.

[6] J. A. Schrock *et al.*, "Failure Analysis of 1200-V/150-A SiC MOSFET Under Repetitive Pulsed Overcurrent Conditions," in *IEEE Transactions on Power Electronics*, vol. 31, no. 3, pp. 1816-1821, March 2016.

[7] J. S. Sullivan and J. R. Stanley, "Wide Bandgap Extrinsic Photoconductive Switches," in *IEEE Transactions on Plasma Science*, vol. 36, no. 5, pp. 2528-2532, Oct. 2008.

[8] W. Shi, C. Ma and M. Li, "Research on the Failure Mechanism of High-Power GaAs PCSS," in *IEEE Transactions on Power Electronics*, vol. 30, no. 5, pp. 2427-2434, May 2015.